

Self-assembly of silver polymers based on flexible isonicotinate ligand at different pH values: syntheses, structures and photoluminescent properties

Feng-Tong Xie^{a,b}, Hai-Ying Bie^a, Li-Mei Duan^a, Guang-Hua Li^a, Xiao Zhang^a,
Ji-Qing Xu^{a,*}

^aState Key Laboratory of Inorganic Synthesis and Preparative Chemistry, College of Chemistry, Jilin University, Changchun 130023, PR China

^bThe Institute of Products Quality and Metrology Inspection of Tongliao City, Tongliao, 028000, China

Received 17 April 2005; received in revised form 29 May 2005; accepted 5 June 2005

Abstract

Two interesting coordination polymers, $[\text{Ag}_8(\text{IN})_6(\text{NO}_3)_2]$ **1** and $[\text{Ag}(\text{IN})(\text{HIN})]_{1/2} [\text{Ag}(\text{IN})]$ **2** (HIN = isonicotinic acid) have been synthesized hydrothermally at different pH values. **1** crystallizes in the triclinic space group $P-1$, with $a = 10.987(2) \text{ \AA}$, $b = 11.625(2) \text{ \AA}$, $c = 17.323(4) \text{ \AA}$, $\alpha = 75.87(3)^\circ$, $\beta = 80.87(3)^\circ$, $\gamma = 76.50(3)^\circ$, $V = 2074.0(7) \text{ \AA}^3$ and $Z = 2$. Compound **1** is the first example of a bilayer framework, in which both single layers are connected by the bond interactions (Ag–O) between Ag from two two-dimensional (2D) single layers generated by the A building block and O atoms from one-dimensional (1D) chain constructed by the B building block, in which coordination modes of IN were reported for the first time. **2** crystallizes in the monoclinic space group $P2(1)/c$, with $a = 8.1668(16) \text{ \AA}$, $b = 19.611(4) \text{ \AA}$, $c = 7.4083(15) \text{ \AA}$, $\beta = 92.90(3)^\circ$, $V = 1185.0(4)$ and $Z = 4$. Compound **2** exhibits a 2D plywood-like structure assembled by hydrogen bonds and weak Ag–O interactions.

© 2005 Elsevier Inc. All rights reserved.

Keywords: Hydrothermal synthesis; Silver; Isonicotinic acid; Coordination polymers; Fluorescence

1. Introduction

In recent years, much attention has been paid to the design and syntheses of metal-organic coordination polymers, due to their intriguing topological structures and potential applications in sorption, electrical conductivity, catalysis and optics, etc [1]. In construction of these extended structures, ligand geometry and coordination preference of the metal ions play important roles, which has been proved by the literatures of a large number of silver coordination polymers [2]. Generally, silver (I) ion adopts linear, trigonal and tetrahedral coordination environments. It has high affinity for hard donor atoms, such as N-donor and/or O-donor atoms,

and soft donor atoms, such as S-donor atoms, being a favorable building block for constructing the framework of coordination polymers [3]. Moreover, the silver ion is prone to form attractive Ag–Ag ligand-supported and ligand-unsupported interactions, such as dimeric structures, polymeric chains and two-dimensional (2D) sheets, etc [3a,4]. It has been proved that different short Ag–Ag interactions are one of the most important factors contributing to the fascinating properties of coordination polymers. For instance, the silver thiolate polymer $[\text{Ag}(\text{C}_5\text{H}_4\text{NS})]_n$, consisting of graphite-like Ag_6 motifs, shows semi-conductivity [3a]. Most references have shown that heterocycle aromatic carboxylic acids, such as isonicotinic acid, are a good candidate for the construction of metal-organic coordination polymers because of their rich coordination modes [5]. Moreover, self-assembly of the silver coordination polymer is

*Corresponding author. Fax: +86 431 8499158.
E-mail address: xjq@mail.jlu.edu.cn (J.-Q. Xu).

highly influenced by the solvent system, template, pH value of the solution and the steric requirement of the counterion [6]. Keeping in mind the above-mentioned issues, by employing the hydrothermal technique, we have successfully isolated two different silver (I)-isonicotinate polymers $[\text{Ag}_8(\text{IN})_6(\text{NO}_3)_2]$ **1** and $[\text{Ag}(\text{IN})(\text{HIN})]_{1/2}[\text{Ag}(\text{IN})]$ **2** (HIN = isonicotinic acid) by tuning pH levels of the solution, both of which display strong fluorescent emissions at room temperature. To the best of our knowledge, **1** is the first example of a bilayer structure in which both single layers are connected by the Ag–O bond interactions between Ag from two 2D single layers generated by the A building block and O atoms from one-dimensional (1D) chain constructed by the B building block, in which IN exhibits novel coordination modes.

2. Experimental section

2.1. Materials and physical methods

All the chemicals were obtained from commercial sources and used without further purification. Infrared spectra were recorded as KBr plates by using a Perkin–Elmer Spectrometer in the 400–4000 cm^{-1} region. Elemental analyses (CHN) were determined using a Perkin–Elmer 2400 LS II elemental analyzer. Fluorescent properties were measured using FS900 Edinburgh instrument. Powder X-ray diffraction (XRD) data were obtained using SHIMADZU XRD-6000 diffractometer with Cu $K\alpha$ radiation ($\lambda = 1.5418 \text{ \AA}$), with step size and count time of 0.02° and 4 s, respectively.

Synthesis of $[\text{Ag}_8(\text{IN})_6(\text{NO}_3)_2]$ (1**):** Compound **1** was synthesized hydrothermally in polytetrafluoroethylene-lined stainless steel autoclaves under autogenous pressure. The reaction of AgNO_3 , HIN, imidazole and H_2O in a molar ratio of 1:1:1:450 was allowed to proceed at 170°C for 4 days (pH = 5), and then the reactant mixture was cooled at room temperature. Buff crystals of **1** (yield 60%) were collected by mechanical isolation and washed with water. $\text{C}_{36}\text{H}_{24}\text{Ag}_8\text{N}_8\text{O}_{18}$ (Mr = 1719.59): calcd. (%) C, 25.15; H, 1.41; N, 6.52; found C, 25.10; H, 1.39; N, 6.64. IR (KBr, cm^{-1}): 3432(m), 1605(s), 1549(s), 1385(s), 1225(w), 1057(w), 1016(w), 865(w), 845(m), 766(s), 702(m), 688(s), 556(w), 508(w), 442(w), 402(w).

Synthesis of $[\text{Ag}(\text{IN})(\text{HIN})]_{1/2}[\text{Ag}(\text{IN})]$ (2**):** Compound **2** was prepared as for **1** performing the similar above-mentioned reaction at pH = 3. Yellow crystals of **2** were obtained (yield 70%). $\text{C}_{12}\text{H}_{8.50}\text{Ag}_{1.50}\text{N}_2\text{O}_4$ (Mr = 406.51): calcd. (%) C, 35.46; H 2.11; N, 6.89; found C, 35.55; H, 2.10; N, 6.82. IR (KBr, cm^{-1}): 3428(m), 1711(s), 1606(s), 1549(s), 1394(s), 1335(m), 1226(w),

1029(w), 866(w), 844(m), 765(s), 702(s), 689(s), 495(m), 422(w), 403(w).

2.2. X-ray crystallography

X-ray single-crystal data collections for **1** and **2** were carried out at 293 K on a Siemens SMART system equipped with a CCD detector with Mo $K\alpha$ radiation at 0.71073 \AA . Empirical absorption corrections were applied using SADABS. The structures were solved by direct methods using SHELXTL programs and refined with the full-matrix least-squares technique. Anisotropic thermal parameters were applied to all non-hydrogen atoms; the organic hydrogen atoms were generated geometrically. The crystallographic data for **1** and **2** are given in Table 1, and the selected bond lengths and angles are listed in Table 2.

3. Results and discussion

3.1. Synthesis and characterization

Because the coordination polymers formed by silver and carboxylate ligands usually appear as insoluble salts at conventional conditions, it makes the structural analyses difficult. It is well known that the hydrothermal technique can provide the environment of high temperature and high pressure, at which the solubility of silver salts increased. Therefore, the hydrothermal reaction can be applied to the design and syntheses of silver coordination polymers.

To our knowledge, isonicotinate, as a potential polydentate ligand, can bridge metal centers together using both the N-donors from pyridine rings and O-donors from the carboxylate [5]. Hence a variety of transition metal (such as Cu, Zn, Cd, etc.) coordination complexes have been reported. Moreover, as demonstrated before, it is possible to control the deprotonation of hydrogen atoms attached to the oxygen atoms of carboxylic groups at different pH levels and hence tune the coordination modes. These facts encouraged us to employ such a potential polydentate ligand by controlling the solution acidity to obtain new silver coordination polymers. The results have shown that the pH levels of the solution play a key role in synthesizing compounds **1** and **2**. At the low pH value (pH = 3), only parts of hydrogen atoms attached to carboxylic groups from HIN have been deprotonated and compound **2** was formed. However, when pH value increased to 5, all hydrogen atoms from carboxylic groups were deprotonated and compound **1** was constructed. It should be pointed out that the same compound **2** as that reported previously was obtained, although a different synthesis method was employed [7]. In this system, imidazole was used in constructing

Table 1
Crystallographic data and structure refinement for compounds **1** and **2**

	1	2
Empirical formula	C ₃₆ H ₂₄ Ag ₈ N ₈ O ₁₈	C ₁₂ H _{8.50} Ag _{1.50} N ₂ O ₄
Formula weight	1719.59	406.51
Crystal system	Triclinic	Monoclinic
Space group	<i>P</i> -1	<i>P</i> 2 (1)/ <i>c</i>
Unit cell dimension	<i>a</i> = 10.987(2) Å α = 75.87(3)° <i>b</i> = 11.625(2) Å β = 80.87(3)° <i>c</i> = 17.323(4) Å γ = 76.50(3)°	<i>a</i> = 8.1668(16) Å <i>b</i> = 19.611(4) Å, β = 92.90(3)° <i>c</i> = 7.4083(15) Å
Volume, <i>Z</i>	2074.0(7) Å ³ , 2	1185.0(4), 4
Density	2.754 g/cm ³	2.279 g/cm ³
<i>F</i> ₍₀₀₀₎	1632	788
Absorption coefficient	3.785 mm ⁻¹	2.516 mm ⁻¹
Crystal size	0.40 × 0.30 × 0.20 mm ³	0.26 × 0.20 × 0.14 mm ³
θ range	3.09–27.48°	3.25–27.46°
Limiting indices	−13 ≤ <i>h</i> ≤ 13, −14 ≤ <i>k</i> ≤ 14, −22 ≤ <i>l</i> ≤ 22	−10 ≤ <i>h</i> ≤ 10, −24 ≤ <i>k</i> ≤ 25, −9 ≤ <i>l</i> ≤ 9
<i>T</i> (K)	293 (2)	293 (2)
Data/restraints/parameters	8003/0/631	2698/0/191
Goodness of fit indicator	0.944	1.152
Final <i>R</i> indicates [<i>I</i> > 2σ(<i>I</i>)]	<i>R</i> ₁ = 0.0481, <i>wR</i> ₂ = 0.1480	<i>R</i> ₁ = 0.0232, <i>wR</i> ₂ = 0.0540
Largest diff. peak and hole	1.412 and −1.428 e/Å ³	0.546 and −0.689 e/Å ³

compounds **1** and **2**. However, no imidazole was found as ligands or guests in the resulting polymer architectures. When the syntheses of compounds **1** and **2** were performed in the absence of imidazole, no single crystals suitable for diffraction analysis were obtained. This fact suggests that imidazole plays a template or structure-directing role in the construction of the resulting coordination structures.

This work demonstrates that the appropriate choice of reaction condition systems and the application of the hydrothermal technique may lead to different silver polymers (Scheme 1).

3.2. Description of the structures

[Ag₈(IN)₆(NO₃)₂] **1**. The structure determination reveals that compound **1** comprises two different building units [Ag₆(IN)₄] (A) and [Ag₂(IN)₂] (B) as shown in Fig. 1. All the carboxylic groups are converted to carboxylates by a deprotonated process, which can be proved by the C–O distances and the infrared spectrum. In the building block A, there are four crystallographically independent IN anions, which adopt the same coordination modes— μ_3 -coordination, as shown in Scheme 2, 1(a). Each IN anion binds to one silver (I) ion by one nitrogen atom from the pyridine ring and the other two silver centers by two oxygen atoms from one carboxylate with *syn-syn* modes. This bridging mode (μ_3 -) of isonicotinate in coordination with the Ag(I) ion is rarely documented. There are six crystallographically independent silver atoms, in which Ag(1), Ag(3), Ag(5) and Ag(7) are three-coordinate by two oxygen atoms and one nitrogen atom from

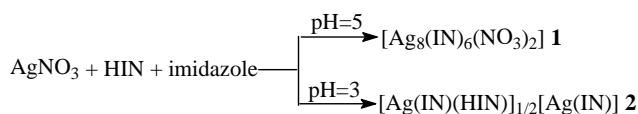
three different ligands with similar average Ag–O distances, being 2.344, 2.323, 2.339 and 2.337 Å, and similar Ag–N distances [2.174(9), 2.185(9), 2.156(8) and 2.159(8) Å] (Fig. 1). The Ag(2) center is two-coordinate by two oxygen atoms from two different ligands with the average Ag–O distance of 2.267 Å. The Ag(6) is three-coordinate by three oxygen atoms from three different ligands with Ag–O_{av} distance of 2.368 Å. It should be noted that there exist Ag–Ag interactions in the unit bridged by one carboxylate group, with Ag(1)–Ag(2), Ag(2)–Ag(3), Ag(5)–Ag(6) and Ag(6)–Ag(7) distances of 3.2986(16), 3.2290(19), 3.2820(19) and 3.2457(16) Å, respectively. Thus, these six silver ions are connected by IN ligands to form a 2D layer, as shown in Fig. 2. It is worth noting that in this 2D layer, there exists a large cavity including six metals. It should be pointed out that there is no interpenetration between adjacent layers.

In the building block B, there are two crystallographically independent silver atoms named Ag(4) and Ag(8), and two IN anions. Both silver atoms adopt Y-shape three-coordinate environments, with two oxygen atoms from the same ligand and one nitrogen atom from the other ligand. The IN anions exhibit two different coordination modes, which are shown in Scheme 2 1(b) and 1(c). One is μ_5 - and the other is μ_4 -coordination modes, both which exhibit novel coordination modes of IN. Moreover, the coordination mode of carboxylates to the Ag(I) ion is rarely documented. As shown in Fig. 3, both of IN ligands chelated to one silver atom by two oxygen atoms from one carboxylate and bridged the other silver atom by nitrogen atom to form a 1D chain.

Table 2
Selected bond lengths (Å) and angles (°) for compounds **1** and **2**

1			
Ag(1)–O(1)	2.118(8)	Ag(1)–O(10)#3	2.569(8)
Ag(1)–N(2)	2.174(9)	Ag(1)–Ag(2)	3.2986(16)
Ag(2)–O(2)	2.263(8)	Ag(2)–O(5)	2.270(8)
Ag(3)–O(6)	2.135(7)	Ag(3)–O(7)	2.509(8)
Ag(3)–N(6)#2	2.185(9)	Ag(3)–Ag(2)	3.2290(19)
Ag(4)–O(7)	2.378(8)	Ag(4)–O(8)	2.448(8)
Ag(4)–N(5)	2.163(9)	Ag(5)–O(4)#3	2.105(7)
Ag(5)–O(8)	2.571(8)	Ag(5)–N(1)#4	2.156(8)
Ag(5)–Ag(6)	3.2820(19)	Ag(6)–O(11)	2.258(8)
Ag(6)–O(3)#3	2.261(8)	Ag(6)–O(8)	2.584(8)
Ag(7)–O(12)	2.130(7)	Ag(7)–O(9)#1	2.542(9)
Ag(7)–N(3)#1	2.159(8)	Ag(7)–Ag(6)	3.2457(16)
Ag(8)#5–N(4)	2.162(9)	Ag(8)–O(10)	2.423(8)
Ag(8)–O(9)	2.429(8)	O(1)–Ag(1)–N(2)	167.2(4)
O(1)–Ag(1)–O(10)#3	104.5(3)	N(2)–Ag(1)–O(10)#3	88.3(3)
O(2)–Ag(2)–O(5)	134.0(4)	Ag(3)–Ag(2)–Ag(1)	116.33(5)
O(6)–Ag(3)–N(6)#2	161.5(4)	O(6)–Ag(3)–O(7)	102.2(3)
N(6)#2–Ag(3)–O(7)	94.2(3)	N(5)–Ag(4)–O(7)	155.8(3)
N(5)–Ag(4)–O(8)	149.8(3)	O(7)–Ag(4)–O(8)	54.3(3)
O(4)#3–Ag(5)–N(1)#4	169.8(4)	O(4)#3–Ag(5)–O(8)	98.5(3)
N(1)#4–Ag(5)–O(8)	91.0(3)	O(11)–Ag(6)–O(3)#3	131.5(4)
O(11)–Ag(6)–O(8)	95.5(3)	O(3)#3–Ag(6)–O(8)	100.5(3)
Ag(7)–Ag(6)–Ag(5)	113.71(5)	O(12)–Ag(7)–N(3)#1	161.1(3)
O(12)–Ag(7)–O(9)#1	100.3(3)	N(3)#1–Ag(7)–O(9)#1	95.7(3)
N(4)#6–Ag(8)–O(10)	150.6(4)	N(4)#6–Ag(8)–O(9)	154.4(4)
O(10)–Ag(8)–O(9)	55.0(3)	Ag(4)–O(8)–Ag(5)	108.3(3)
Ag(4)–O(8)–Ag(6)	90.2(2)	Ag(5)–O(8)–Ag(6)	79.1(2)
Ag(4)–O(7)–Ag(3)	110.7(3)	Ag(8)–O(10)–Ag(1)#3	107.1(3)
Ag(8)–O(9)–Ag(7)#1	112.3(3)		
2			
Ag(1)–N(1)	2.1434(19)	Ag(1)–N(1)#1	2.1434(19)
Ag(2)–N(2)	2.171(2)	Ag(2)–O(3)	2.1332(18)
N(1)–Ag(1)–N(1)#1	180.0	O(3)–Ag(2)–N(2)	155.75(8)

Symmetry transformations used to generate equivalent atoms for **1**: #1 $-x+2, -y+1, -z+1$; #2 $-x+2, -y, -z+2$; #3 $-x+1, -y+1, -z+1$; #4 $-x+1, -y, -z+2$; #5 $x, y-1, z+1$; #6 $x, y+1, z-1$; for **2**: #1 $-x, -y+1, -z-1$.



Scheme 1. The reaction conditions of **1** and **2**.

Then the two neighboring 2D single layers are connected together by the bond interactions (Ag–O) between the Ag from two single layers and O of μ_5 - and μ_4 - IN from 1D chains to form the novel 2D bilayer structure (Fig. 4). It should be noted that Ag–O bonds such as O10–Ag1, O9–Ag7, O8–Ag5, O8–Ag6, O7–Ag3 play pivotal roles in constructing this bilayer structure. In comparison with the previously reported bilayers, the construction mode of this kind of bilayer is firstly observed. Thus, if the interactions of the neighbouring layers are omitted, a wheel-like 2D structure is constructed, as exhibited in Fig. 4(b). It should be pointed out that the extension direction of the 1D chain

is in accordance with the 2D bilayers, so the structure of **1** is still 2D not 3D.

The crystal structure of **1** exhibits more intriguing features in contrast to the previous report about the Ag–IN polymer, $[\text{Ag}_4(\text{IN})_4 \cdot \text{H}_2\text{O} \cdot 0.5\text{CH}_3\text{OH}]_n$ **3** [7]. Although both compounds exhibit a novel 2D bilayer structure, their construction modes are different. In **1** the bilayer is generated by Ag–O bond interactions between two 2D single layers and interesting 1D chain, and this construction mode is reported firstly. In **3**, it is constructed by Ag–Ag interactions. In addition, the 2D single layers in both compounds are constructed by different building blocks. In **1**, it is constructed by the $[\text{Ag}_6(\text{IN})_4]$ building block (A), in which three silver atoms formed linear Ag–Ag interactions. However, in **3** 2D layers are constructed by $[\text{Ag}_4(\text{IN})_4]$ building block, in which only two silver atoms formed Ag–Ag interactions. The sizes of cavities in **1** consisting of six silver atoms are obviously larger than the square-grid-type cavities only comprising four silver atoms in **3**.

Furthermore, the coordination modes of IN ligands are more versatile and interesting in **1**, found to be μ_3 , μ_4 , μ_5 -coordinate, which exhibits the novel coordination modes.

$[Ag(IN)(HIN)]_{1/2}[Ag(IN)]$ (**2**). Because of the influence of the pH values, only part of the carboxylic groups converted carboxylates by a deprotonated

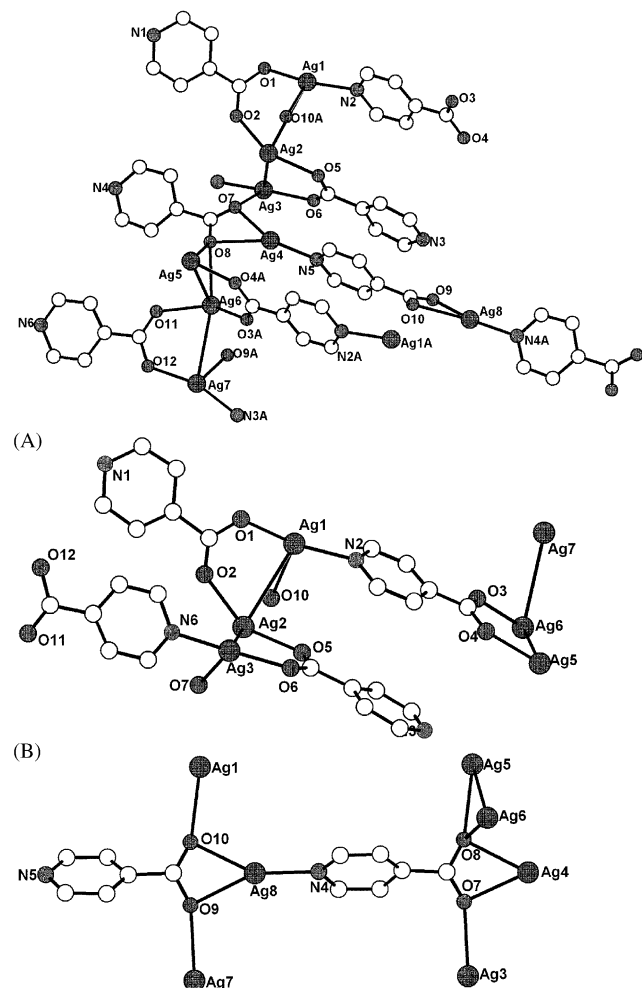


Fig. 1. The coordination modes of IN ligands and the environments of silver ions in compound **1**: (A) shows the building block A; (B) exhibits the building block B.

process, and IN only exhibits μ_1 - and μ_2 - coordination modes. The structure analysis reveals that compound **2** consists of two different 1D chains, in which one is constructed by the A building unit $[Ag(IN)(HIN)]$ through self-assembly hydrogen bonds interactions (Fig. 5(a)) and the other is built by the B building block $[Ag(IN)]$ (Fig. 5(b)).

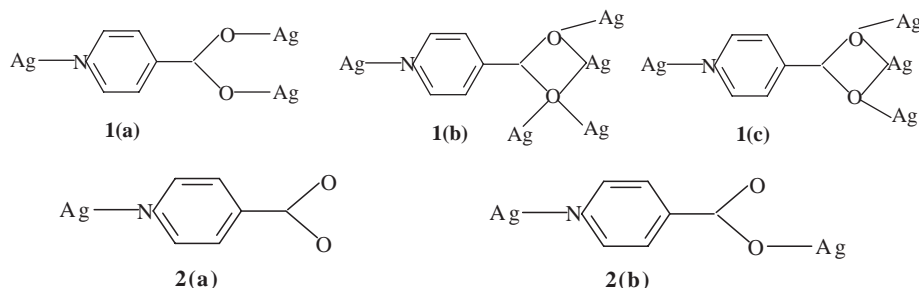
In the A building block, silver(I) ion adopts a linear coordination with two nitrogen atoms from one HIN molecule and one IN anion. The IN is coordinated to only one silver ion by its nitrogen atom, and its coordination modes are shown in Scheme 2, 2(a). This metallic building block is assembled to a 1D chain by hydrogen bonds between one carboxylate and the other neighboring carboxylic group.

In the B building block, silver(I) adopts a distorted linear coordination geometry with one nitrogen atom from pyridine ring and one oxygen atom from mono-dentate carboxylate. The IN anion is coordinated to two silver ions by its nitrogen atoms and oxygen atom to form a 1D chain, and its coordination modes are shown in Scheme 2, 2(b). There exist strong Ag–O interactions between A and B 1D chains $[Ag1 \cdots O4$ 2.865(5) Å and $Ag2 \cdots O1$ 2.662(2) Å], which make two different 1D chains to be connected to form the plywood-like structures [8].

Powder XRD pattern for **1** was consistent with the simulated one on the basis of the single-crystal structure, as shown in Fig. 6. The diffraction peaks on both patterns corresponded well in position, indicating the phase purity of the as-synthesized sample. The difference in reflection intensities between the simulated and experimental patterns was due to the variation in crystal orientation for the powder sample.

3.3. Spectroscopic investigations

In general the IR spectra show features attributable to each component of the complexes. For complex **1**, the characteristic bands of the carboxylate are shown in the usual region at 1549 cm^{-1} (vs) for the antisymmetric stretching and at 1385 cm^{-1} (s) for symmetric stretching [9]. The separation (Δ) between $\nu_{as}(\text{CO}_2)$ and $\nu_{sym}(\text{CO}_2)$



Scheme 2. The coordination modes of the isonicotinate ligands in compounds **1** and **2**.

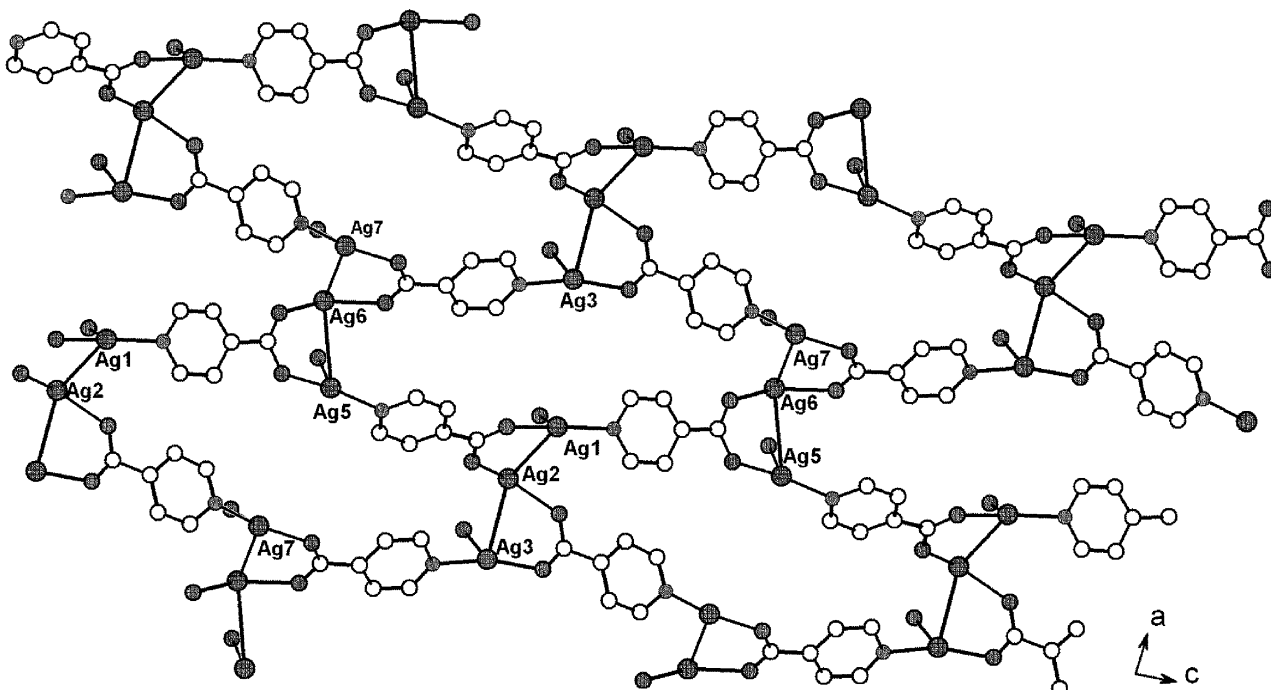


Fig. 2. The two-dimensional single layer structure constructed by the building block A in compound 1.

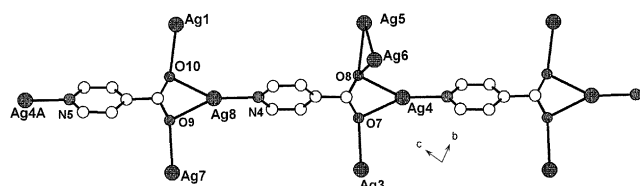


Fig. 3. The one-dimensional chain constructed by the building block B in compound 1.

is 164 cm^{-1} . For complex 2, the characteristic bands of the carboxylate are shown at 1549 cm^{-1} (vs) for the antisymmetric stretching and at 1394 cm^{-1} (vs) for symmetric stretching. The Δ value of complex 2 is 155 cm^{-1} . In addition, in compound 2, one strong absorption at 1711 cm^{-1} can be attributed to the protonated carboxylic double bond [10], showing that HIN molecules are not deprotonated completely. The split of $\nu_{\text{as}}(\text{CO}_2)$ in both complexes indicates that the carboxylates exhibit different coordination fashions (Scheme 2), in agreement with their crystal structures.

3.4. Fluorescent properties

Most luminescent Ag(I) compounds exhibit weak emission at low temperature. Some important examples are organometallic silver(I) compounds containing bridging acetylide ligands [11], silver(I) diisocyanide [12] and other silver(I) cyanide compounds [13]. Only a few monomeric and polymeric Ag(I) complexes exhibit luminescence at room temperature. Interestingly, both

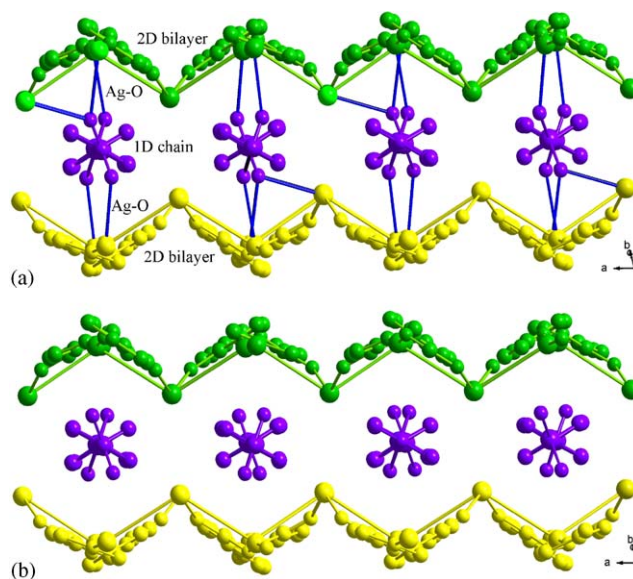


Fig. 4. (a) The 2D bilayer structures of compound 1; (b) the wheel-like structures when the Ag–O bonds connecting 2D single layers and 1D chain together are omitted.

compounds 1 and 2 exhibit luminescent properties at ambient temperature. The emission spectra of 1–2 at room temperature in the solid state are shown in Fig. 7. It can be observed that one strong emission approximately occurs at 364 nm ($\lambda_{\text{ex}} = 300\text{ nm}$) for 1, which should be assigned to neither LMCT (ligand-to-metal charge transfer) nor MLCT (metal-to-ligand charge

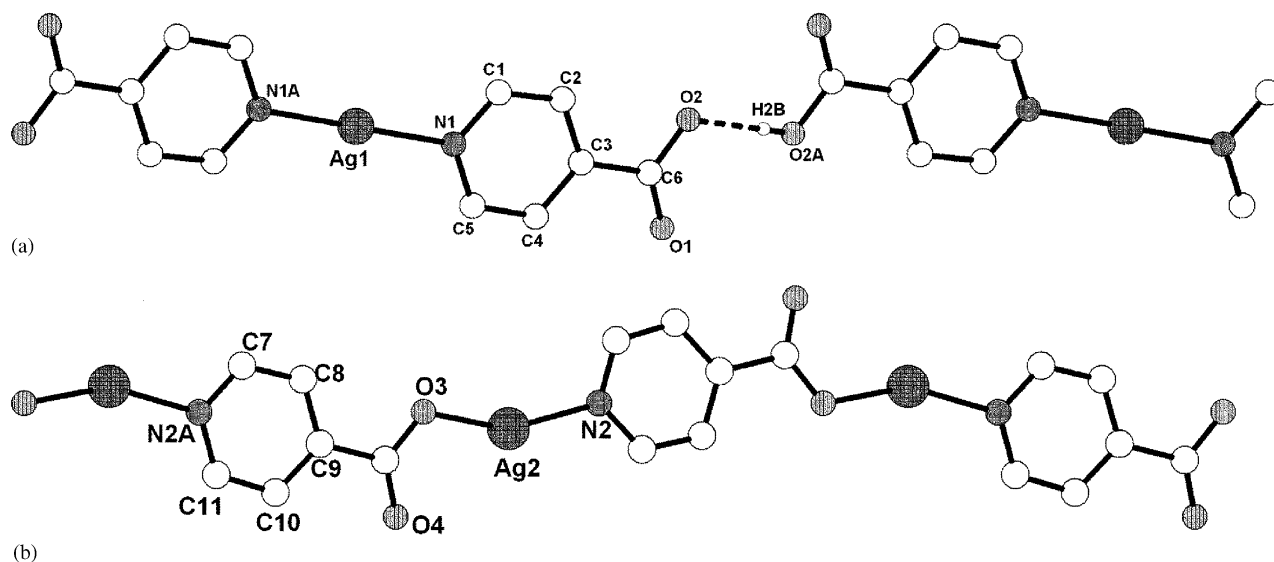


Fig. 5. Two different one-dimensional chains observed in crystal structure of **2**. (a) The A building unit is self-assembly by O–H...O hydrogen bonds; (b) Plot of 1D extended structure of the B building block.

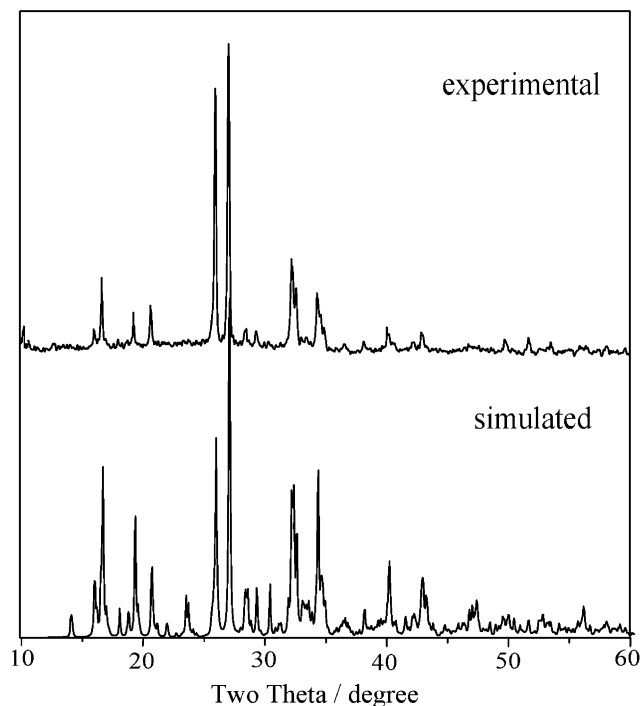


Fig. 6. Experimental and simulated powder X-ray diffraction patterns for **1**.

transfer) in nature and can probably be assigned to intraligand fluorescent emission, since free IN molecules exhibit a similar fluorescent emission at 369 nm ($\lambda_{\text{ex}} = 220$ nm). In addition, solid **1** also exhibits one strong emission at 531 nm upon excitation at 450 nm. It has been suggested that the emissions in the reported

silver (I) complexes originate either from $d\sigma^* - p\sigma$, $4d - 5s$ transitions, or from the charge transfer between metal and ligand. For **1**, a possible assignment for the origin of the emission involves emissive states derived from LMCT transition mixed with $d-s$ character [6]. Presumably, in complex **1**, the highest occupied molecular orbital (HOMO) is associated with the silver(I) $4d$ orbital and the carboxylate group σ orbital, while the lowest unoccupied molecular orbitals (LUMOs) are mainly associated with silver(I) unoccupied hybrid orbital based on $4d$, $5s$ and $5p$. The diagram of energy levels for **1** can be drawn according to the fluorescent property. When excited at 300 nm, the electron transfers from ground state E_0 to excited state E_4 , then it non-radiatively decays to E_3 energy level, from which it comes back to ground state E_0 with light energy emission (364 nm). When excited at 450 nm, the electron transfers from ground state E_0 to excited state E_2 . Then the excitation energy non-radiatively decays to E_1 energy levels with the green photoluminescence.

The emission band of **2** exhibits one strong peak at 364 nm ($\lambda_{\text{ex}} = 300$ nm), which is similar to that of **1** and can be assigned to the intraligand electronic transition, and two weak peaks at 400 and 486 nm ($\lambda_{\text{ex}} = 234$ nm), which is probably due to the $L \rightarrow M$ charge-transfer transition because there is no emission peak at this position for the free ligand. In comparison with compound **2**, the strong emission of **1** from the charge transfer between ligand and metal may be attributed to the Ag–Ag interactions, which may result in the different HOMO–LUMO gaps. This fact demonstrated that direct metal–metal interactions may be one of the important factors contributing to the photoluminescent

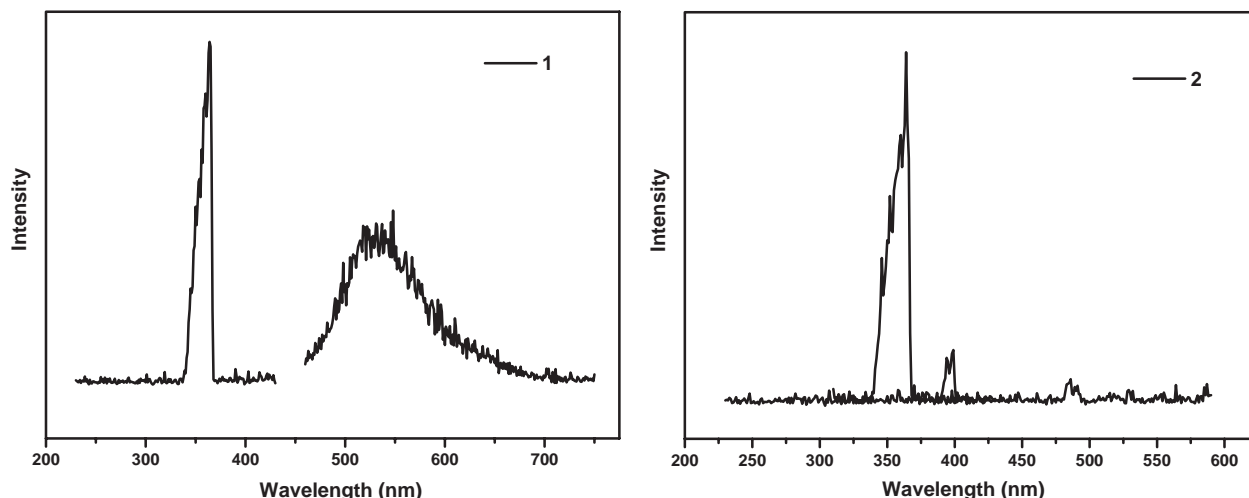


Fig. 7. The fluorescent emission spectra of **1** and **2** in the solid state at room temperature.

properties of coinage d^{10} metal coordination compounds. When excited at 300 nm, the electron transfers from ground state E0 to excited state E4, then it non-radiatively decays to E3 energy levels, from which it comes back to ground state E0 with light energy emission (364 nm), the same to **1**. When excited at 234 nm, the electron transfers from ground state E0 to excited state E5, then it non-radiatively decays to E2 and E1 energy levels, from which it comes back to ground state E0 with weak energy emission (400 and 486 nm). It is verified by the fluorescent spectrum that the non-radiative decay in this process is very strong and caused the weak blue light observed.

The fluorescent spectra of **1** and **2** were also measured in DMF solutions, as shown in Fig. 8. For both **1** and **2**, there are two strong emission peaks at 315 and 345 nm upon excitation at approximately 210 nm, which should be the $\pi-\pi^*$ electronic transfer of free IN intraligand. There is no emission peak that can be caused by electronic transfer between the metal and ligands as in the solid state. This implies that the polymers disaggregate into oligomers in DMF solutions. Further work on this subject is in progress.

In summary, we present two photoluminescent 2D coordination polymers constructed with AgNO_3 and HIN molecules. Compound **1** is the first example of a bilayer framework, in which both single layers are connected by the bond interactions (Ag–O) between Ag from two 2D single layers generated by the A building block and O atoms from 1D chain constructed by the B building block, in which coordination modes of IN are firstly reported. Compound **2** exhibits a 2D plywood-like structure assembled by hydrogen bonds and weak Ag–O interactions. The isolation of **1** and **2** demonstrates that the pH values play an important role in the self-assembly process of both architectures.

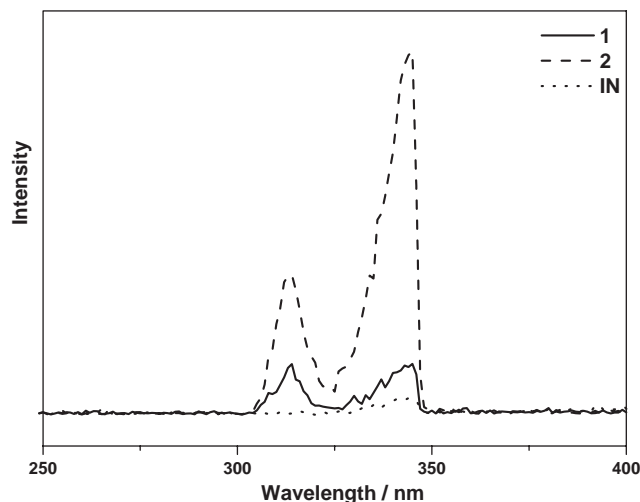


Fig. 8. The fluorescent emission spectra of **1**, **2** and IN in DMF solutions at room temperature.

Supplementary data

Supplementary data have been deposited with the Cambridge Crystallographic Centre, CCDC No. 232368 and 232369. Copy of this information may be obtained free of charge from The Director, CCDC, 12 Union Road, Cambridge, CB2 1EZ, UK (fax: +44 1223 336033; e-mail: deposit@ccdc.cam.ac.uk or [www: http://www.ccdc.cam.ac.uk](http://www.ccdc.cam.ac.uk)).

Acknowledgments

This research was supported by grants from the National Natural Science Foundation of China (No. 20271021 and No. 20333070).

References

- [1] (a) K.S. Min, M.P. Suh, *J. Am. Chem. Soc.* 122 (2000) 6834;
(b) S. Kondo, M. Kitagawa, K. Seki, *Angew. Chem., Int. Ed.* 39 (2000) 2082;
(c) M. Eddaoudi, D.B. Moler, H. Li, B. Chen, T.M. Reineke, M. O’Keeffe, O.M. Yaghi, *Acc. Chem. Res.* 34 (2001) 319.
- [2] (a) D. Sun, R. Cao, W. Bi, J. Weng, M. Hong, Y. Liang, *Inorg. Chim. Acta* 357 (2004) 991;
(b) S.L. Zheng, M.L. Tong, X.L. Yu, X.M. Chen, *J. Chem. Soc., Dalton Trans.* (2001) 586;
(c) D. Sun, R. Cao, W. Bi, X. Li, Y. Wang, M. Hong, *Eur. J. Inorg. Chem.* (2004) 2144.
- [3] (a) W. Su, M. Hong, J. Weng, R. Cao, S. Lu, *Angew. Chem. Int. Ed.* (39) (2000) 2911;
(b) P. Vaquero, A.M. Chippindale, A.R. Cowley, A.V. Powell, *Inorg. Chem.* 42 (2003) 7846;
(c) A.P. Côté, G.K.H. Shimizu, *Inorg. Chem.* 43 (2004) 6663;
(d) Q.M. Wang, T.C.W. Mak, *Inorg. Chem.* 42 (2003) 1637;
(e) S.L. Zheng, M.L. Tong, R.W. Fu, X.M. Chen, S.W. Ng, *Inorg. Chem.* 40 (2001) 3562;
(f) S.L. Zheng, M.L. Tong, X.M. Chen, S.W. Ng, *J. Chem. Soc., Dalton Trans.* (2002) 360.
- [4] (a) M.L. Tong, X.M. Chen, B.H. Ye, *Inorg. Chem.* 37 (1998) 5278;
(b) K. Singh, J.R. Long, P. Stavropoulos, *J. Am. Chem. Soc.* 119 (1997) 2942;
(c) X.M. Ming, T.C.W. Mak, *J. Am. Chem. Soc.* (1991) 3253;
(d) O. Kristiansson, *Inorg. Chem.* 40 (2001) 5058;
(e) C.N.R. Rao, A. Ranganathan, V.R. Pedireddi, A.R. Raju, *Chem. Commun.* (2000) 39.
- [5] (a) M.E. Chapman, P. Ayyappan, B.M. Foxman, G.T. Yee, W. Lin, *Cryst. Growth Des.* (2001) 159;
(b) M.L. Tong, L.J. Li, K. Mochizuki, H.C. Chang, X.M. Chen, Y. Li, S. Kitagawa, *Chem. Commun.* (2003) 428;
(c) C.Z.J. Lin, S.S.Y. Chui, S.M.F. Lo, F.L.Y. Shek, M. Wu, K. Suwinska, J. Lipkowski, I.D. Williams, *Chem. Commun.* (2002) 1642;
(d) J.H. Yu, J.Q. Xu, L. Ye, H. Ding, W.J. Jing, T.G. Wang, J.N. Xu, H.B. Xu, Z.C. Mu, G.D. Yang, *Inorg. Chem. Commun.* 5 (2002) 572;
(e) J.H. Liao, C.Y. Lai, C.D. Ho, C.T. Su, *Inorg. Chem. Commun.* 7 (2004) 402.
- [6] J.H. Yang, S.L. Zheng, X.L. Yu, X.M. Chen, *Cryst. Growth Des.* (2004) 831.
- [7] Z. Liu, P. Liu, Y. Chen, J. Wang, M. Huang, *New J. Chem.* 29 (2005) 474.
- [8] B. Cova, A. Briceño, R. Atencio, *New J. Chem.* 25 (2001) 1516.
- [9] (a) C.G. Zheng, Y.L. Xie, R.G. Xiong, X.Z. You, *Inorg. Chem. Commun.* 4 (2001) 405;
(b) H.Y. Bie, J.H. Yu, K. Zhao, J. Lu, L.M. Duan, J.Q. Xu, *J. Mol. Struct.* 741 (2005) 77.
- [10] Z.Y. Fu, X.T. Wu, J.C. Dai, S.M. Hu, W.X. Du, H.H. Zhang, R.Q. Sun, *Eur. J. Inorg. Chem.* (2002) 2730.
- [11] V.W.W. Yam, K.K.W. Lo, W.K.M. Fung, C.R. Wang, *Coord. Chem. Rev.* 171 (1998) 17.
- [12] P.D. Harvey, D. Fortin, *Coord. Chem. Rev.* 171 (1998) 351.
- [13] M.A. Omary, H.H. Patterson, *J. Am. Chem. Soc.* 120 (1998) 7696.